RSC Advances

RSC Publishing

COMMUNICATION

View Article Online
View Journal | View Issue

Metal incorporated Horseradish Peroxidase (HRP) catalyzed oxidation of resveratrol: selective dimerization or decomposition†

Cite this: *RSC Adv.*, 2013, **3**, 22976

Received 19th July 2013
Accepted 30th September 2013

DOI: 10.1039/c3ra43784a

www.rsc.org/advances

Chang Li, Xiaofei Xu, Jing Lu, Lin Wang and Yuanjiang Pan*

Horseradish Peroxidase (HRP) is a commercially available and prevalently used peroxidase with no specific substrate binding domain. However, after being incorporated with different metal cations, new catalytic functions were found in biomimetic oxidation of resveratrol. Based on the results of screening, Ca, Cu, Fe and Mn incorporated enzymes showed distinctive effects, either decomposition or dimerization products were observed.

With diverse beneficial activities for human health, resveratrol (**1**) was considered an attractive small organic molecule by the pharmaceutical industry in the first decade of this century.[1] Meanwhile, naturally occuring resveratrol oligomers could be considered as a series of analogues built from several resveratrol molecules with complicated linkage type. Up to now, more than 500 these oligomers have been isolated from plants, especially *vitis* plants. Resveratrol oligomers also have various impressive bioactivities, but few progresses have been made due to their trace amount in natural resources.[2] Synthesis of resveratrol oligomers, both total synthesis[3] and biomimetic synthesis,[4] have been put forward in great steps during last five years, and the related researches have been well reviewed.[5]

As most resveratrol oligomers are oxidative coupling products generated from monomers, searching for suitable oxidants is not only necessary but also of significant scientific value. After numerous efforts for a long history, redox-active enzymes are proved effective. Screening for 'good' enzymes was performed by several researchers before. In these processes, selected enzyme was put into a stock of resveratrol solution, and the products were separated with chromatographic methods. A few enzymes, including laccase,[6a] *Momordica charantia* peroxidase[6b] and tyrosinase,[6c] have been carefully examined. Among them horseradish peroxidase (HRP, EC 1.11.1.7) is the most effective one, which has high efficiency and bulk resource. HRP was first introduced into resveratrol oxidation by Langcake and Pryce in 1977.[7] In most cases, hydroperoxide plays as the final oxidant in reaction, which could be converted into hydroxyl radical in presence of HRP.[8] Water–acetone co-solvent system is preferred in moderate temperature while *trans*-δ-viniferin (**2**) and pallidol (**5**) could be found in a complicated reaction mixture. However, low conversion and lack of selectivity is the major drawback of this enzymatic reaction. Considering these challenges, efforts were devoted to regulate the catalytic behavior of HRP in this reaction. Hou and coworkers used a modified resveratrol with two *tert*-butyl groups adjacent to the hydroxyl group in the phenol ring as a substrate and quadrangularin A was selectively obtained in 35% yield.[9] Our group have also provided some resolutions, where the resveratrol monomer was replaced by its natural oligomers, to perform [n + 1] reactions to get oligomers in higher oligomeric degree.[10] For instance, parthenocissin A (a resveratrol dimer) reacted with resveratrol to generate laetevirenol E (a resveratrol trimer).[10a] We have also provided an enzymatic resolution strategy.[11] pH environment of this reaction was carefully adjusted, by which three different catalytic modes were switched concisely to form seven different resveratrol dimers selectively.

On the other hand, it is a new cross point in biocatalysis to expand the reaction horizon of a specific enzyme by some developed strategies,[12] such as mutagenesis,[13a] amino acid substitution[13b] or computational design.[13c] Among them, metal incorporation is the one of the most concise pathways. Some approaches were made, including direct metal substitution,[14a] metal incorporation[14b] and conjugation of artificial metal complex.[14c] Most of these approaches were focused on some model organic reactions, while very few efforts have been put in practical reactions, especially in natural product synthesis, whose biomimetic synthesis still faces great challenges.

Herein, we explored the potential function of several metal incorporated HRPs in this specific catalysis, in order to find if this strategy could help to get oxidative products different from native HPR catalyzed reaction. After screening of seven M^{2+} ions

Department of Chemistry, Zhejiang University, Hangzhou, 310027, P. R. China. E-mail: panyuanjiang@zju.edu.cn; Fax: +86 571 87951629; Tel: +86 571 87951629

† Electronic supplementary information (ESI) available. See DOI: 10.1039/c3ra43784a

in behavior change of HRP, it was found that they have diverse effects on this biomimetic transition (Fig. 1). Either decomposition or dimerization products were isolated in some cases, while others metals have negative or no influence on HRP's catalytic behavior.

In present study, seven different M^{2+} ions (corresponding chloride salts, 240 μM) were incubated with HRP in 25 μM aqueous solution under 40 °C for 12 hours. After thorough dialysis and lyophilization, the formed metal incorporated enzymes were used instead of HRP in a developed protocol as what we have described in previous research.[11] The other difference was that water was applied other than buffer. pH was testified both before and after enzymatic reactions, and the results distributed between 6.8 and 7.1, which indicates the reaction here is metal-dependent rather than pH-dependent as in our former report.[11] The reaction products were carefully examined with HPLC and some of them were further isolated using chromatographic methods. The results turned to be in great variance (HPLC chromatograms were shown in Fig. 3, for yields and other details, see Table S1 in ESI†). Ni^{2+}, Co^{2+} and Zn^{2+} brought out no significant effect on HRP's catalytic mode (Scheme 1A, Fig. 2 and Fig. 3B). As in a typical resveratrol oxidative reaction catalyzed be native HRP, *trans*-δ-viniferin (**2**) was found as the main product in around 60% yield. Leachianol F and leachianol G (**3** & **4**, a pair of diasteroisomers in 1 : 2 ratio) and pallidol (**5**) were also isolated as byproducts. Meanwhile, incorporation of Ca^{2+} could decrease the catalytic capacity of HRP, the conversion of resveratrol decreased by 40% and enzyme sedimentation was observed (Scheme 1B and Fig. 3C). HRP–Mn^{2+} complex give *trans*-δ-viniferin as a solo-product in 91% yield, without any byproduct concominantly formed (Scheme 1C and Fig. 3D). Moreover, two other transition metals, Cu^{2+} and Fe^{2+}, also showed interesting results that decompositive oxidation occurred to resveratrol. The C–C double bond of resveratrol was cleaved, and its two sides suffered an asymmetric oxidation. The final products of this decompositive oxidation isolated were identified 4-hydroxybenzylaldehyde (**6**, around 70% yield) and 3,5-dihydroxybenzylacid (**7**, around 50% yield). (Scheme 1D and Fig. 3E). Thus, incorporation of metal ions made a fork in HRP's normal catalytic pathway, at which resveratrol can go through either a dimerizative road in high efficiency with Mn^{2+}, or a decompositive oxidative one in presence of Cu^{2+} or Fe^{2+}.

To further investigate the details of how these phenomena were achieved, three groups of control experiments were designed. In the first array of trials, the common oxidative products (as suggested in both our[11] and other researchers'[7]

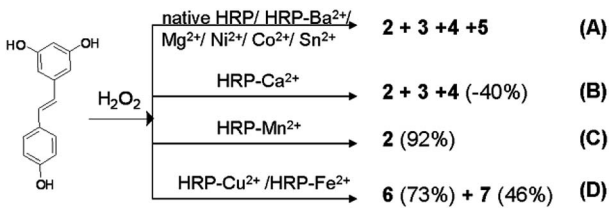

Scheme 1 M^{2+} incorporated HRP catalyzed resveratrol oxidation.

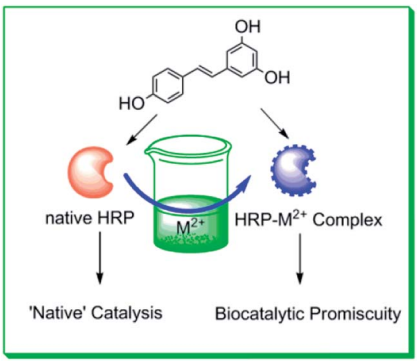

Fig. 1 Metal ions regulate modes of HRP catalysis in resveratrol oxidation.

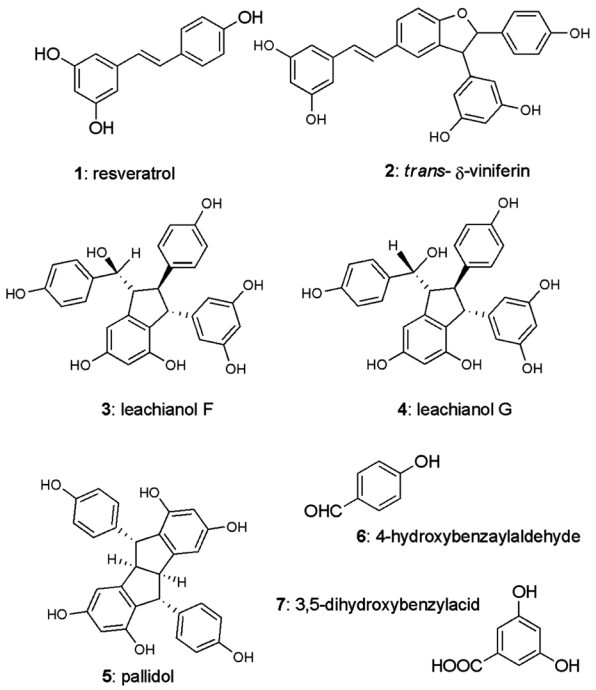

Fig. 2 Compounds appeared in this research.

previous works), *trans*-δ-viniferin (**2**), was subjected as reactant in presence of HRP, [HRP–Fe], [HRP–Cu] or [HRP–Mn]. (Entry 1–4, Table 1.) After reacted with H_2O_2 under the standard reaction condition, the products were checked both with HPLC and NMR. However, no reaction seems to happen in this process. Thus, it is indicated that **2** was not formed as an intermediate in the catalytic process with HRP–metal complexes. Then the catalytic capabilities of the metals (only the ones with specific function were analyzed, they are Fe, Cu and Mn complexes) alone were tested in absence of HRP. (Entry 5–7, Table 1) The results showed that these three metals all have considerable catalytic capacities in dimerizing resveratrol (**1**) to **2** in presence of H_2O_2. It is mentionable that in $FeCl_2$ catalyzed transformation, the yield of **2** is over 90%, which is in accordance with Tanaka's previous work[9] using $FeCl_3$ as oxidant. But in all the forementioned entries, neither decompositive products (**6** and **7**) nor other dimerization products (**3**, **4** and **5**) could

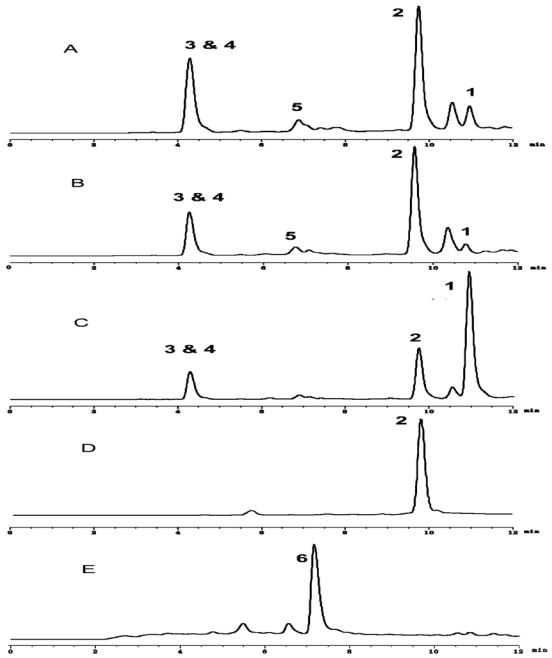

Fig. 3 HPLC chromatograms of HRP–metal complexes catalyzed products. The catalysts used are (A) native HRP. (B) Co^{2+} incorporated HRP (the same as Ni^{2+} and Zn^{2+} cases). (C) Ca^{2+} incorporated HRP. (D) Mn^{2+} incorporated HRP. (E) Fe^{2+} incorporated HRP (the ethyl acetate extraction, the same as Cu^{2+} incorporated HRP). HPLC condition, see ESI.†

Table 1 Results of control experiments with different treatment to HRP

Entry	Catalyst	Substrate	Product & yield
1	HRP	**2**	No reaction
2	[HRP–Fe]	**2**	No reaction
3	[HRP–Cu]	**2**	No reaction
4	[HRP–Mn]	**2**	No reaction
5	$FeCl_2$	Resveratrol (**1**)	**2**, 92%
6	$CuCl_2$	Resveratrol (**1**)	**2**, 85%
7	$MnCl_2$	Resveratrol (**1**)	**2**, 51%
8	*apo*-HRP	Resveratrol (**1**)	No reaction
9	[*apo*-HRP–Fe]	Resveratrol (**1**)	No reaction
10	[*apo*-HRP–Cu]	Resveratrol (**1**)	No reaction
11	[*apo*-HRP–Mn]	Resveratrol (**1**)	No reaction

be found in HPLC and NMR analysis. These results identified that HRP was involved in the reactions and incorporation with it dramatically changed the catalytic behaviors of these metal ions. Furthermore, it is well known that HRP is a 34 kD protein conjugated with a heme prosthetic group. So the function of heme was also studied in this research. *apo*-HRP was prepared within classic methods,[15] and incubated with $FeCl_2$, $CuCl_2$ and $MnCl_2$ respectively to form [*apo*-HRP–metal] complexes. These complexes were also utilized in resveratrol oxidation under H_2O_2 after dialyzation. (Entry 8–11, Table 1) It was found that none of them can catalyze resveratrol oxidation. It could be proposed from these phenomena that the heme centre of HRP is the hinge of the initial conversion of hydroperoxide to hydroxyl radical, which further lead to the formation of a phenol radical intermediate. And all products, either

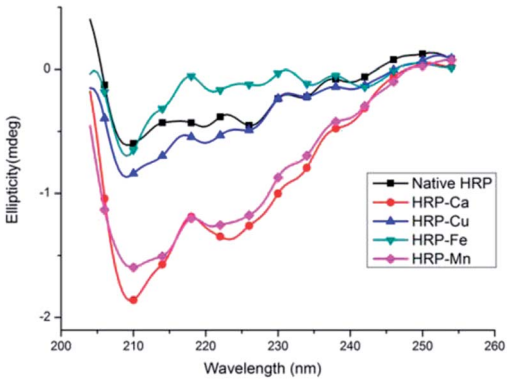

Fig. 4 Far-UV CD spectra of native HRP, [HRP–Ca], [HRP–Cu], [HRP–Fe] and [HRP–Mn].

dimerization products or decomposition products are generated from the phenol radical.

These interesting phenomena suggest that the enzyme itself underwent some changes in property. Further analysis was carried out in order to understand the mechanistic reason and provide more instructive information to artificial HRP design, further analysis was carried out to reveal a deeper insight. Atomic absorption spectrometry (AAS) was applied to count the enzyme–metal ratios in the formed complexes. Thoroughly dialyzed and lyophilized metal incorporated HRPs were solved in water and their corresponding metal ions were detected. The results (see in ESI†) suggest that [HRP–Mn_{11}], [HRP–Cu_6] and [HRP–Fe_3] were formed in these examples.

Circular dichroism, a sensitive and convenient way to check the conformational change of a given protein,[16] was also used to characterize the differences between different artificial M^{2+} incorporated HRPs (only the ones with specific function were analyzed, those are [HRP–Mn], [HRP–Fe] and [HRP–Cu]) and native HRP. It has been proved that negative CD signals at 209 nm and 222 nm are typical features of protein containing α-helical structure, [17] which is the main constitution of HRP's secondary structure.[18] However, the results showed that there's significant substantial changes occur in the CD band at 222 nm and 209 nm (Fig. 4) to various degrees. [HRP–Ca] and [HRP–Mn] have more intense change, indicating the enzyme conformation changed a lot after binding to metal ions, which leads to unfolding of α-helix. At the mean time, [HRP–Fe] and [HRP–Cu] suffered less difference compared with native HRP, therein binding of iron or copper ion to HRP is proposed to form new reactive sites on the surface of protein rather than to change the conformation of enzyme. Upon the results above, it could be hypothesized that these metal ions (Mn^{2+}, Cu^{2+}, and Fe^{2+}) can be incorporated to native HRP and cause conformational change, which further leads to the functional change of HRP.

Conclusion

As conclusion, a novel concise protocol to synthesize versatile oxidative products from resveratrol was developed. Using metal incorporated HRP as catalyst, resveratrol oxidation could be

performed in 'selective' ways. Among them, *trans*-δ-viniferin was obtained in 91% yield when catalyzed by [HRP–Mn_{11}], and C=C bond cleavage was found in presence of [HRP–Cu_6] or [HRP–Fe_3]. Initial mechanistic analysis of these 'man-made' HRP–metal complexes was also carried out using circular dichroism (CD) and Atomic Absorption Spectrometry (AAS).

Experimental section

General procedures

All reagents were purchased at the highest commercial quality and used without further purification. Reactions were magnetically stirred and monitored by thin-layer chromatography (TLC) or high performance liquid chromatography (HPLC). HPLC analysis was carried out using a C18 column (250 mm × 4.6 mm i.d., 5 μm). Purification of compounds was carried out with silica gel (academic grade, 200–300) and a preparative HPLC (C18 column, 250 × 20 mm i.d). NMR spectra were recorded on a 500 MHz instrument. Mass spectroscopic data were obtained using oa-TOF mass spectrometer.

Generation of M^{2+} incorporated HRPs

Aqueous solution of HRP was prepared in concentration of 1 mg mL^{-1}. All metal chloride solutions were prepared in concentration of 10 μM. For a M^{2+} incorporated HRP generation, 3 mL of HRP solution was mixed with 3 mL metal chloride solution, well shaken, and then incubated for 24 hours. Dialysis was then carried out with dialysis tube (M_W = 3500) in deionized water. After 72 hours, the dialyzed solution was then lyophilized at −70 °C.

Generation of M^{2+} incorporated *apo*-HRP

apo-HRP was prepared following the reported procedure.[17] To generate M^{2+} incorporated *apo*-HRP, the same procedure as forementioned one was carried out, except that *apo*-HRP was used instead of HRP.

Horseradish peroxidase catalyzed oxidation of 1

A mixture of **1** (0.4 mmol, 91.2 mg) and M^{2+} incorporated HRP (160 μL, 1 mg mL^{-1} aqueous solution) was added to a mixed solvent consisted of 2 mL acetone and 2 mL water. This solution was then stirred at 40 °C for one hour. Then 60 μL fresh 30% H_2O_2 was then added to the solution. After one hour, the reaction was quenched by saturated $Na_2S_2O_3$ solution, evaporated, and extracted with EtOAc and water. The organic layer was washed by brine and water for three times, dried over anhydrous sodium sulphate and concentrated.

Metal chlorides catalyzed oxidation of 1

To make it as control, this oxidation was carried out following the procedures of HRP catalyzed oxidation, where HRP was replaced by metal chlorides ($FeCl_2$, $CuCl_2$ and $MnCl_2$ in 0.04 mmol).

M^{2+} incorporated HRP catalyzed oxidation of 2

The oxidation procedure was the same as HRP catalyzed oxidation of **1**.

Product analysis and separation

Analysis of the product solution was carried out on HPLC with a C-18 column (column temperature, 25 °C; mobile phase, methanol and water at the gradient: methanol, 0–8 min, 40–53%, 8–15 min, 53%, 15–20 min, 53–90%; flow rate, 0.8 mL min^{-1}; detection, 280 nm UV). HPLC yields were calculated by peak area, assuming all the products share the same absorption at 280 nm. Separation was carried out on a preparative HPLC with a C-18 column, using gradient elution (methanol, 0–24 min, 40–53%; 24–40 min, 53%; 40–60 min, 53–90%) and detected at 280 nm UV. Separations were only carried out in some of the reactions ([HRP–Mn], [HRP–Fe], [HRP–Cu] and native HRP). A Sephadex LH-20 gel column was occupied together with a preparative HPLC to purify the products. The yields of corresponding products in different reactions were listed in Table S1, ESI.†

The analysis data of products are listed and the NMR spectra are in the end of ESI.†

trans-δ-Viniferin (**2**) was obtained as a yellow amorphous powder. ^{1}H NMR (500 MHz, acetone) δ 8.48 (s, 1H), 8.24 (s, 2H), 8.20 (s, 2H), 7.44 (d, J = 5.0 Hz, 1H), 7.26 (m, 3H), 7.06 (d, J = 15.0 Hz, 1H), 6.92 (d, J = 15.0 Hz, 1H), 6.87 (m, 3H), 6.55 (d, 2H), 6.28 (d, J = 10.0 Hz, 2H), 6.20 (d, J = 5.0 Hz, 2H), 5.46 (d, J = 5.0 Hz, 1H), 4.48 (d, J = 5.0 Hz, 1H); ^{13}C NMR (125 MHz, acetone) δ 160.6, 159.7, 159.5, 158.4, 145.2, 140.8, 132.5, 132.1, 131.7, 129.1, 128.6, 127.2, 123.9, 116.2, 110.1, 107.4, 105.7, 102.7, 102.3, 94.0, 57.8, 55.4. HRMS(EI) calcd for $C_{28}H_{22}O_6^+$ [M^+] 454.1416, found 454.1414.

Leachianol F (**3**) and leachianol G (**4**) was obtained as a brown amorphous powder. The product got was a 1 : 2 mixture. Data of 3: ^{1}H NMR (500 MHz, acetone) δ 7.99 (br, 5H), 7.47 (s, 1H), 6.84–6.88 (m, 4H), 6.70–6.73 (m, 2H), 6.67 (d, J = 5.0 Hz, 2H), 6.58 (d, 1H), 6.30 (d, J = 5.0 Hz, 1H), 6.12 (m, 1H), 5.92 (d, 1H), 4.48 (m, 1H), 4.22 (d, J = 5.0 Hz, 1H), 4.08 (d, J = 5.0 Hz, 1H), 3.36 (m, 1H), 2.94 (t, J = 5.0 Hz, 1H); ^{13}C NMR (125 MHz, acetone) δ 159.1, 158.8, 157.1, 156.3, 155.0, 150.6, 148.7, 137.4, 136.1, 129.3, 128.8, 122.5, 115.6, 115.4, 106.1, 106.0, 102.4, 101.2, 76.6, 61.8, 59.4, 55.6. HRMS(EI) calcd for $C_{28}H_{24}O_7^+$ [$(M - H_2O)^+$] 454.1416, found 454.1419. Data of 4: ^{1}H NMR (500 MHz, acetone) δ 8.10 (br, 5H), 7.44 (s, 1H), 7.07 (d, J = 10.0, 2H), 6.85 (m, 2H), 6.67 (m, 4H), 6.22 (d, 2H), 6.16 (d, 2H), 6.14 (d, J = 5.0 Hz, 2H), 5.74 (d, J = 5.0 Hz, 1H), 4.48 (m, 1H), 4.26 (d, 1H), 4.14 (d, 1H), 3.48 (t, J = 5.0 Hz, 1H), 3.40 (m, 1H); ^{13}C NMR (125 MHz, acetone) δ 159.2, 158.5, 157.2, 156.2, 154.8, 151.4, 147.3, 138.0, 135.7, 129.4, 129.3, 106.2, 105.6, 102.4, 101.0, 77.3, 62.5, 59.0, 56.0. HRMS(EI) calcd for $C_{28}H_{24}O_7^+$ [$(M - H_2O)^+$] 454.1419, found 454.1419.

Pallidol (**5**) was obtained as a brown amorphous powder. ^{1}H NMR (500 MHz, acetone) δ 8.19 (s, 2H), 8.15 (s, 2H), 7.92 (s, 2H), 7.05 (d, J = 10.0 Hz, 4H), 6.77 (d, J = 10.0 Hz, 4H), 6.70 (s, 2H), 6.26 (s, 2H), 4.63 (s, 2H), 3.88 (s, 2H); ^{13}C NMR (125 MHz, acetone) δ 159.0, 155.1, 150.2, 137.6, 129.0, 123.2, 115.8, 103.3,

102.4, 60.3, 53.8. HRMS(EI) calcd for $C_{28}H_{22}O_6^+$ [M^+] 454.1416, found 454.1417.

4-Hydroxybenzylaldehyde (**6**) was obtained as a white amorphous powder. ^{1}H NMR (500 MHz, DMSO) δ 10.62 (s, 1H), 9.79 (s, 1H), 7.76 (d, J = 5.0 Hz, 2H), 6.94 (d, J = 10.0 Hz, 2H); ^{13}C NMR (125 MHz, DMSO) δ 190.9, 163.3, 132.1, 128.4, 115.8.

3,5-Dihydroxybenzylacid (**7**) was obtained as a white amorphous powder. ^{1}H NMR (500 MHz, DMSO) δ 12.67 (s, 1H), 9.55 (s, 2H), 6.81 (d, 2H), 6.42 (s, 1H); ^{13}C NMR (125 MHz, DMSO) δ 167.3, 158.4, 132.5, 107.3, 106.8.

Characterization of M^{2+} incorporated HRPs' conformation with circular dichroism spectrometer

1 mg lyophilized M^{2+} incorporated HRPs were solved in 2 mL water. A spectrometer was used for CD spectroscopy, spectra were recorded at 25 °C, using a path length of 1.0 cm. Spectra were recorded in the range of 200–300 nm.

Determination of M^{2+} incorporated HRPs' constitution with atomic absorption spectrometer (AAS)

4 mg lyophilized M^{2+} incorporated HRPs were solved in 2 mL water. An atomic absorption spectrometer was applied, the test conditions are as follows. Current 6 mA/0 mA, 6 mA/500 mA; burner height 7 mm; wave length 324.8 nm; burner angle 0 deg; slit width 0.5 nm; fuel gas flow 1.8 L min^{-1}; lighting mode BGC-D_2, BGC-SR; type of oxidant air. The results were listed in Table S3, ESI.†

Acknowledgements

Financial support from National Basic Research Program of China (973 program, 2011CB710800) and Joint Sino-German Research Project GZ689 is gratefully acknowledged.

Notes and references

1 (*a*) J. A. Baur and D. A. Sinclair, *Nat. Rev. Drug Discovery*, 2006, **5**, 493–506; (*b*) S. Quideau, D. Deffieux, C. Douat-Casassus and L. Pouysegu, *Angew. Chem., Int. Ed.*, 2011, **50**, 586–621.

2 T. Shen, X. N. Wang and H. X. Lou, *Nat. Prod. Rep.*, 2009, **26**, 916–935.

3 For selected references in total synthesis, see (*a*) S. A. Snyder, A. Gollner and M. I. Chiriac, *Nature*, 2011, **474**, 461–466; (*b*) S. A. Snyder, S. B. Thomas, A. C. Mayer and S. P. Breazzano, *Angew. Chem., Int. Ed.*, 2012, **51**, 4080–4084.

4 For selected references in biomimetic synthesis, see (*a*) M. Sako, H. Hosokawa, T. Ito and M. I. Iinuma, *J. Org. Chem.*, 2004, **69**, 2598–2600; (*b*) S. S. Velu, I. Buniyamin, L. K. Ching, F. Feroz, I. Noorbatcha, L. C. Gee, K. Awang, I. A. Wahab and J. F. F. Weber, *Chem.– Eur. J.*, 2008, **14**, 11376–11384.

5 S. A. Snyder, A. M. ElSohly and F. Kontes, *Nat. Prod. Rep.*, 2011, **28**, 897–924.

6 (*a*) C. Ponzoni, E. Beneventi, M. R. Cramarossa, S. Raimondi, G. Trevisi, U. M. Pagnoni, S. Riva and L. Forti, *Adv. Synth. Catal.*, 2007, **349**, 1497–1506; (*b*) C. F. Xie, H. Q. Yuan, J. B. Qu, J. Xing, B. B. Lu, X. N. Wang, M. Ji and H. X. Lou, *Chem. Biodiversity*, 2009, **6**, 1193–1201; (*c*) N. Lee, E. J. Kim and B. G. Kim, *ACS Chem. Biol.*, 2012, **7**, 1687–1692.

7 P. Langcake and R. J. Pryce, *J. Chem. Soc. Chem. Commun.*, 1977, 208–210.

8 Y. Takaya, K. Terashima, J. Ito, Y. H. He, M. Tateoka, N. Yamaguchi and M. Niwa, *Tetrahedron*, 2005, **61**, 10285–10290.

9 W. L. Li, H. Li, Y. Li and Z. J. Hou, *Angew. Chem., Int. Ed.*, 2006, **45**, 7609–7611.

10 (*a*) S. He, B. Wu, Y. J. Pan and L. Y. Jiang, *J. Org. Chem.*, 2008, **73**, 5233–5241; (*b*) L. Y. Jiang, S. He, C. R. Sun and Y. J. Pan, *Phytochemistry*, 2012, **77**, 294–303.

11 C. Li, J. Lu, X. F. Xu, R. L. Hu and Y. J. Pan, *Green Chem.*, 2012, **14**, 3281–3284.

12 (*a*) P. Grunwald, *Biocatalysis – Biochemical Fundamental and Applications*, Imperial College Press, Singapore, 2009; (*b*) M. S. Humble and P. Berglund, *Eur. J. Org. Chem.*, 2011, 3391–3401; (*c*) P. J. Deuss, R. den Heeten, W. Laan and P. C. J. Kamer, *Chem.– Eur. J.*, 2011, **17**, 4680–4698.

13 (*a*) J. Podtetenieff, A. Taglieber, E. Bill, E. J. Reijerse and M. T. Reetz, *Angew. Chem., Int. Ed.*, 2010, **49**, 5151–5155; (*b*) H. Jochens, K. Stiba, C. Savile, R. Fujii, J. G. Yu, T. Gerassenkov, R. J. Kazlauskas and U. T. Bornscheuer, *Angew. Chem., Int. Ed.*, 2009, **48**, 3532–3535; (*c*) D. Rothlisberger, O. Khersonsky, A. M. Wollacott, L. Jiang, J. DeChancie, J. Betker, J. L. Gallaher, E. A. Althoff, A. Zanghellini, O. Dym, S. Albeck, K. N. Houk, D. S. Tawfik and D. Baker, *Nature*, 2008, **453**, 190–194.

14 (*a*) K. Okrasa and R. J. Kazlauskas, *Chem.– Eur. J.*, 2006, **12**, 1587–1596; (*b*) F. van de Velde, L. Könemann, F. van Rantwijk and R. A. Sheldon, *Chem. Commun.*, 1998, 1891–1892; (*c*) M. T. Reetz and N. Jiao, *Angew. Chem., Int. Ed.*, 2006, **45**, 2416–2419.

15 T. Ueno, M. Ohashi, M. Kono, K. Kondo, A. Suzuki, T. Yamane and Y. Watanabe, *Inorg. Chem.*, 2004, **43**, 2852–2858.

16 B. M. Dunn, D. W. Speicher, P. T. Wingfield and J. E. Coligan, *Short Protocols in Protein Science*, Wiley-VCH Verlag GmbH & Co. KGaA, Weinheim, 2003.

17 (*a*) Y. P. Myer, *J. Biol. Chem.*, 1968, **243**, 2115–2122; (*b*) J. Tang, J. Jiang, Y. Song, Z. Peng, Z. Wu, S. Dong and E. Wang, *Chem. Phys. Lipids*, 2002, **120**, 119–129.

18 M. Gajhede, D. J. Schuller, A. Henriksen, A. T. Smith and T. L. Poulos, *Nat. Struct. Biol.*, 1997, **4**, 1032–1038.

